J|A|C|S
ARTICLES

Published on Web 03/21/2008

An Exploration of Mechanisms for the Transformation of 8-Oxoguanine to Guanidinohydantoin and Spiroiminodihydantoin by Density Functional Theory

Barbara H. Munk,[†] Cynthia J. Burrows,[‡] and H. Bernhard Schlegel*,[†]

Department of Chemistry, Wayne State University, Detroit, Michigan, 48202, and Department of Chemistry, University of Utah, 315 South 1400 East, Salt Lake City, Utah 84112-0850

Received November 19, 2007; E-mail: hbs@chem.wayne.edu

Ⓦ **This paper contains enhanced objects available on the Internet at http://pubs.acs.org/jacs.**

Abstract: The potential energy surface for formation of 2-amino-5-hydroxy-7,9-dihydropurine-6,8-dione (5-OH-OG), guanidinohydantoin (Gh) and spiroiminodihydantoin (Sp) from 8-oxoguanine (8-oxoG) has been mapped out using B3LYP density functional theory, the aug-cc-pVTZ and 6-31+G(d,p) basis sets and the IEF-polarizable continuum model (PCM) solvation model. Three pathways for formation of 5-OH-OG from 8-oxoG were evaluated: (A) stepwise loss of two electrons and two protons to form the quinonoid intermediate 2-amino-7,9-dihydro-purine-6,8-dione (8-oxoG^{ox}) followed by hydration; (B) stepwise loss of two electrons and one proton and net addition of hydroxide, in which the key step is nucleophilic addition to the 8-oxoG radical cation; and (C) stepwise loss of one electron and one proton and addition of hydroxyl radical to the 8-oxoG radical cation. The data suggest that all three pathways are energetically feasible mechanisms for the formation of 5-OH-OG, however, Pathway A may be kinetically favored over Pathway B. Although lower in energy, Pathway C may be of limited biological significance since it depends on the local concentration of hydroxyl radical. Pathways for hydrolysis and decarboxylation of 5-OH-OG to form Gh via either a carboxylic acid or substituted carbamic acid intermediate have been evaluated with the result that cleavage of the N1−C6 bond is clearly favored over that of the C5−C6 bond. Formation of Sp from 5-OH-OG via stepwise proton transfer and acyl migration or ring opening followed by proton transfer and ring closure have also been explored and suggest that deprotonation of the hydroxyl group facilitates a 1,2 acyl shift. Results of the calculations are consistent with experimental studies showing dependence of the Gh/Sp product ratio on pH. Under neutral and basic conditions, the data predict that formation of Sp is kinetically favored over the pathways for formation of Gh. Under acidic conditions, Gh is predicted to be the kinetically favored product.

Introduction

Oxidative damage to DNA has been studied extensively in the last few decades as it is thought to be responsible for a variety of biological sequelae including cancer, cell aging and death.[1–4] Guanine is the most easily oxidized of the DNA bases, and its oxidation leads to the production of a variety of products including 8-oxo-7,8-dihydro-2′-deoxyguanine (8-oxoG, **1**). This lesion is estimated to be generated at the rate of approximately 2000 lesions per human cell per day.[5,6] 8-oxoG is more susceptible to oxidation than the original guanine nucleobase,[7] although identification of 8-oxoG's secondary oxidation products is complicated by the plethora of pathways available to this highly functionalized heterocycle. Ultimately, spiroiminodihydantoin (Sp, **21**) and guanidinohydantoin (Gh, **12**) emerged as two of the major products, both of which are thought to be formed via a common intermediate, 5-hydroxy-8-oxo-7,8-dihydroguanosine (5-OH-OG, **6**) (Scheme 1).[8,9]

The oxidation of 8-oxoG, **1**, has been studied by a number of experimental groups[8–27] and is commonly more easily oxidized in single-stranded versus duplex DNA. Further, dif-

[†] Wayne State University.
[‡] University of Utah.

(1) Gimisis, T.; Cismas, C. *Eur. J. Org. Chem.* **2006**, 1351–1378.
(2) Burrows, C. J.; Muller, J. G. *Chem. Rev.* **1998**, *98*, 1109–1151.
(3) Breen, A. P.; Murphy, J. A. *Free Radical Biol. Med.* **1995**, *18*, 1033–1077.
(4) Pratviel, G.; Meunier, B. *Chem.-Eur. J.* **2006**, *12*, 6018–6030.
(5) Beckman, K. B.; Ames, B. N. *J. Biol. Chem.* **1997**, *272*, 19633–19636.
(6) Foksinski, M.; Rozalski, R.; Guz, J.; Ruszkowska, B.; Sztukowska, P.; Piwowarski, M.; Klungland, A.; Olinski, R. *Free Radical Biol. Med.* **2004**, *37*, 1449–1454.
(7) Steenken, S.; Jovanovic, S. V.; Bietti, M.; Bernhard, K. *J. Am. Chem. Soc.* **2000**, *122*, 2373–2374.
(8) Luo, W. C.; Muller, J. G.; Rachlin, E. M.; Burrows, C. J. *Chem. Res. Toxicol.* **2001**, *14*, 927–938.
(9) Luo, W. C.; Muller, J. G.; Rachlin, E. M.; Burrows, C. J. *Org. Lett.* **2000**, *2*, 613–616.
(10) Hickerson, R. P.; Prat, F.; Muller, J. G.; Foote, C. S.; Burrows, C. J. *J. Am. Chem. Soc.* **1999**, *121*, 9423–9428.
(11) Cadet, J.; Douki, T.; Gasparutto, D.; Ravanat, J. L. *Mutat. Res.* **2003**, *531*, 5–23.
(12) Hah, S. S.; Kim, H. M.; Sumbad, R. A.; Henderson, P. T. *BioMed. Chem. Lett.* **2005**, *15*, 3627–3631.
(13) Hosford, M. E.; Muller, J. G.; Burrows, C. J. *J. Am. Chem. Soc.* **2004**, *126*, 9540–9541.
(14) Luo, W. C.; Muller, J. G.; Burrows, C. J. *Org. Lett.* **2001**, *3*, 2801–2804.
(15) McCallum, J. E. B.; Kuniyoshi, C. Y.; Foote, C. S. *J. Am. Chem. Soc.* **2004**, *126*, 16777–16782.

Scheme 1. Literature Mechanism for the Transformation of 8-Oxoguanine to guanidinohydantoin and Spiroiminodihydantoin (adapted from refs 8–23)

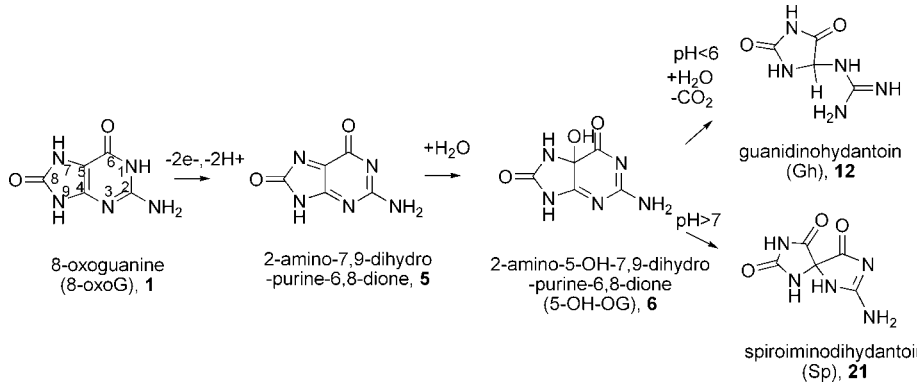

ferent secondary oxidation products are observed depending on the type of oxidant and the pH of the medium. Singlet oxygen was proposed to react with 8-oxoguanine via a [2 + 2] cycloaddition reaction with the C4−C5 double bond.[15] Proton transfer and ring opening of the dioxetane formed via this reaction leads to the formation of 5-hydroperoxy-8-oxoG, which can undergo reduction to the alcohol, **6**, and rearrangement to form Sp, **21**. In nucleosides, one-electron oxidants such as Na_2IrCl_6, and $K_3Fe(CN)_6$, $CoCl_2/KHSO_5$, hydroxyl radical, hydroperoxyl radical, and oxyl radical readily oxidize the purine moiety of 8-oxoG, **1**, producing the two diastereomers of Sp, **21** at neutral or higher pH and two diastereomers of Gh, **12**, at slightly acidic pH.[9] The formation of these two products in oligomers is strongly temperature dependent with Sp, **21**, the predominant product at 50 °C and Gh at 4 °C.[28]

Mechanisms for production of both Sp, **21**, and Gh, **12**, from 8-oxoG, **1**, and guanine have been proposed by a number of researchers.[1,8–10,13,15,18,20,22,23,29] Depending on the oxidizing agent, the proposed mechanisms suggest that 8-oxoG, **1**, undergoes either a one- or two-electron oxidation and concurrent loss of proton(s) followed by nucleophilic addition at the C5 position. What remains unknown is the timing of the events of electron and proton loss with respect to nucleophilic addition, i.e. does water add to 8-oxoG radical cation, **2**, (after one-electron oxidation) or to a quinonoid dehydro-8-oxoG, **5**, that has already undergone 2-electron oxidation?

Addition of the nucleophile at the C5 position has been confirmed using $H_2{}^{18}O$ where mass spectral analysis confirmed 98% incorporation of ^{18}O in the resulting Sp adduct.[9] When water is the nucleophile, the species generated is thought to be 2-amino-5-hydroxy-7,9-dihydropurine-6,8-dione (5-OH-OG, **6**).[8,15] In a study conducted by McCallum et al.,[15] a stable intermediate formed during the oxidation of 8-oxoG, **1**, to Sp, **21**, using singlet oxygen was isolated and characterized using ^{13}C, 2D NMR HMBC spectra conducted at –60 °C, and the structure was assigned to be 5-hydroperoxy-8-oxoG based upon chemical shifts computed at the GIAO/B3LYP/6-311+G(2d,p)//6-31G(d) level of theory. Upon reduction at –40 °C, the formation of 5-OH-OG, **6**, was observed, and its structure was assigned using the same criteria. Upon warming to room temperature, the 5-OH-OG intermediate rearranged to form Sp, **21**. The structure of this final product was confirmed by comparing the NMR and MS/MS spectra of the isolated product with literature values.

Depending on the reaction conditions, 5-OH-OG, **6**, may then rearrange to form Sp, **21**, or hydrate and lose CO_2 to form Gh, **12**. The latter pathway may be similar to that observed for the formation of allantoin from urate which has been the subject of experimental study for decades.[30,31] Urate and allantoin differ from 8-oxoG, **1**, and Gh, **12**, by the substitution of a carbonyl group instead of an amino group at the C2 position of 8-oxoG. In a recent study by Kahn et al.,[31] ^{13}C NMR studies provided evidence that this reaction proceed via an intermediate similar to 5-OH-OG, **6**, which undergoes hydrolysis at the N1−C6 bond before decarboxylation to form allantoin.

In the case of 5-OH-OG, **6**, conversion to Gh, **12**, there is debate in the literature regarding the direction of ring opening of the hydrated species prior to decarboxylation with some mechanisms proposing cleavage of the N1−C6 bond.[8,22] Other proposed mechanisms suggest that the C5−C6 bond is broken to generate a ring-opened carboxyguanidine that decarboxylates to give Gh, **12**.[18,32] Under neutral conditions, the N1−C6 bond is expected to have a higher bond dissociation energy due to delocalization of the nitrogen lone pair electrons. For example, the bond dissociation energy of the carbon−nitrogen bond in acetamide is about 15 kcal/mol higher than the bond dissociation

(16) Joffe, A.; Geacintov, N. E.; Shafirovich, V. *Chem. Res. Toxicol.* **2003**, *16*, 1528–1538.
(17) Misiaszek, R.; Crean, C.; Joffe, A.; Geacintov, N. E.; Shafirovich, V. *Chem. Res. Toxicol.* **2004**, *17*, 1765–1765.
(18) Misiaszek, R.; Crean, C.; Geacintov, N. E.; Shafirovich, V. *J. Am. Chem. Soc.* **2005**, *127*, 2191–2200.
(19) Misiaszek, R.; Crean, C.; Joffe, A.; Geacintov, N. E.; Shafirovich, V. *J. Biol. Chem.* **2004**, *279*, 32106–32115.
(20) Neeley, W. L.; Essigmann, J. M. *Chem. Res. Toxicol.* **2006**, *19*, 491–505.
(21) Niles, J. C.; Wishnok, J. S.; Tannenbaum, S. R. *Org. Lett.* **2001**, *3*, 963–966.
(22) Niles, J. C.; Wishnok, J. S.; Tannenbaum, S. R. *Chem. Res. Toxicol.* **2004**, *17*, 1510–1519.
(23) Ye, Y.; Muller, J. G.; Luo, W. C.; Mayne, C. L.; Shallop, A. J.; Jones, R. A.; Burrows, C. J. *J. Am. Chem. Soc.* **2003**, *125*, 13926–13927.
(24) Yu, H. B.; Venkatarangan, L.; Wishnok, J. S.; Tannenbaum, S. R. *Chem. Res. Toxicol.* **2005**, *18*, 1849–1857.
(25) Niles, J. C.; Wishnok, J. S.; Tannenbaum, S. R. *Nitric Oxide* **2006**, *14*, 109–121.
(26) Niles, J. C.; Venkatarangan, L. M.; Wishnok, J. S.; Tannenbaum, S. R. *Chem. Res. Toxicol.* **2002**, *15*, 1675–1676.
(27) Slade, P. G.; Priestley, N. D.; Sugden, K. D. *Org. Lett.* **2007**, *9*, 4411–4414.
(28) Kornyushyna, O.; Berges, A. M.; Muller, J. G.; Burrows, C. J. *Biochemistry* **2002**, *41*, 15304–15314.
(29) Misiaszek, R.; Uvaydov, Y.; Crean, C.; Geacintov, N. E.; Shafirovich, V. *J. Biol. Chem.* **2005**, *280*, 6293–6300.
(30) Poje, M.; Sokolicmaravic, L. *Tetrahedron* **1988**, *44*, 6723–6728.
(31) Kahn, K.; Serfozo, P.; Tipton, P. A. *J. Am. Chem. Soc.* **1997**, *119*, 5435–5442.
(32) Duarte, V.; Gasparutto, D.; Yamaguchi, L. F.; Ravanat, J. L.; Martinez, G. R.; Medeiros, M. H. G.; Di Mascio, P.; Cadet, J. *J. Am. Chem. Soc.* **2000**, *122*, 12622–12628.

energy of the carbon−carbon bond in acetone.[33] This difference in energy favors cleavage of the C5−C6 bond and may play a role in the preference for acyl migration and formation of Sp, **21**, under neutral conditions. Under acidic conditions, nucleophilic attack at the carbonyl carbon yields a tetrahedral intermediate, and the relative bond energy may shift to favor cleavage of the N1−C6 bond, in part because of the stability of the guanidinium leaving group.

In an effort to clarify the structure of Sp, **21**, researchers have conducted theoretical calculations on certain species in the reaction pathway. McCallum et al. examined the relative enthalpy at 0 K of 4-hydroxy-9-methyl-8-oxoguanine (4-OH-8-oxo-methylG), 5-hydroxy-9-methyl-8-oxoguanine (5-OH-8-oxo-methylG), and 9-methylspiroiminodihydantoin using the B3LYP/6-311+G(2p,d)//B3LYP/6-31G(d) level of theory (zero-point energy scaled by 0.9806). Their calculations indicate that the 4-OH-8-oxo-methylG and 5-OH-8-oxo-methylG adducts are higher in energy than Sp by 31.4 and 18.2 kcal/mol, respectively.[15] Barrier heights for conversion of the alcohols to Sp, **21**, were not reported.

Broyde and Geacintov have conducted several computational studies on the structure and thermodynamics of Sp, **21**.[34–36] QM/MM calculations on the *R* and *S* stereoisomers of Sp nucleosides at the B3LYP/6-31G(d) level of theory in coordination with the Merck molecular force field (MMFF94) provided three-dimensional potential energy surfaces mapping the range and flexibility of the glycosidic torsion angles. Molecular dynamics simulations in 11-mer DNA revealed that the Sp stereoisomers are most likely to be positioned in the B-DNA major groove. The latter studies were carried out using AMBER with the Cornell force field and the PARM99 parameter set. The electrostatic potentials for these studies were computed at the HF/6-31G(d) level of theory with the RESP fitting algorithm. The potential energy surfaces for the mechanism of formation of Sp, **21**, were not discussed by these research groups. The authors suggested that the mutagenicity of the Sp lesions may be due in part to their unusual configuration and hydrogen bonding properties within DNA.

In the present study, we employ density functional methods to complete the first comprehensive evaluation of the energetics of various pathways leading from 8-oxoG, **1**, to Sp, **21**, and Gh, **12**. By mapping the potential energy surface for each pathway, we hope to gain a better understanding of the order of events (i.e., electron loss, proton transfer, hydroxylation at C5) in the oxidation of 8-oxoG, **1**, to 5-OH-OG, **6**. Further, we hope to identify the most likely mechanism for conversion of this intermediate to Gh, **12**, and Sp, **21**. We also explore the energetics for hydrolysis of the C5−C6 bond versus the N1−C6 bond in the pathways leading to Gh, **12**, in an effort to explain the experimentally observed product branching ratios resulting from differences in reaction conditions. The effect of protonation/deprotonation on the relative energies of various intermediates and barrier heights for mechanisms leading to both Gh, **12**, and Sp, **21**, are also described.

Method

Molecular orbital calculations were carried out using the development version of the Gaussian series of programs.[37] Optimized geometries and energies in the gas phase were computed with the B3LYP density functional method[38–40] using the 6-31+G(d,p) basis set[41–46] for nearly all of the reactants, products, and transition states. Our previous computational studies with the 8-hydroxyguanine radical indicated that the potential energy profiles of adducts substituted at N9 with methyl, hydroxymethyl, and methoxyethyl were similar to those observed with hydrogen as the substituent.[47] Therefore, the model compounds for the calculations were the 8-oxoguanine nucleobase with hydrogen as the substituent at N-9.

Transition states involving proton transfer from one adduct to another were modeled with explicit molecules of water assisting the proton transfer. In general, the transition states thus formed were six-membered rather than four-membered ring systems and should therefore represent a lower-energy pathway. Single-point calculations in aqueous solution were carried out at the gas-phase optimized geometry for the adducts and corresponding transition states using the integral equation formalism of the polarizable continuum model (IEF-PCM) at the B3LYP/aug-cc-pVTZ[48] level of theory. With the exception of **22c**, geometry optimizations for all reactants, intermediates, and products along the reaction pathways were carried out in the gas phase. Gas-phase calculations predict that the **22c** zwitterion will form an epoxide at the C4−C5 bond. Gas-phase geometry optimizations were unable to locate the transition state for the acyl migration reactions proposed for the formation of Sp, **21**, from 5-OH-OG, **6**. Therefore, adduct **22c** and the transition states for all of the acyl migration reactions for Pathways G, H, and I [**6/9TS**, **19/20TS**, **22a/21bTS**, **22b/21cTS**, and **22c/21aTS**] were optimized in solution at the IEF-PCM[49–54]//B3LYP/6-31+G(d,p) level of theory.

The computations were conducted with the F01, F02, F02plus, and G01 development versions of the Gaussian suite of programs

(33) *Handbook of Bond Dissociation Energies in Organic Compounds*; Luo, Y.-R., Ed.; CRC Press LLC: Boca Raton, FL, 2003.
(34) Jia, L.; Shafirovich, V.; Shapiro, R.; Geacintov, N. E.; Broyde, S. *Biochemistry* **2005**, *44*, 13342–13353.
(35) Jia, L.; Shafirovich, V.; Shapiro, R.; Geacintov, N. E.; Broyde, S. *Biochemistry* **2005**, *44*, 6043–6051.
(36) Durandin, A.; Jia, L.; Crean, C.; Kolbanovskiy, A.; Ding, S.; Shafirovich, V.; Broyde, S.; Geacintov, N. E. *Chem. Res. Toxicol.* **2006**, *19*, 908–913.
(37) Frisch, M. J.; et al.; *Gaussian Development Version, Revision E.05, F01, F02, and G01 ed.*; Gaussian, Inc.: Wallingford, CT, 2006. See Supporting Information for full ref.
(38) Becke, A. D. *Phys. Rev. A* **1988**, *38*, 3098–3100.
(39) Becke, A. D. *J. Chem. Phys.* **1993**, *98*, 5648–5652.
(40) Lee, C.; Yang, W.; Parr, R. D. *Phys. Rev. B* **1988**, *37*, 785–789.
(41) Ditchfield, R.; Hehre, W. J.; Pople, J. A. *J. Chem. Phys.* **1971**, *54*, 724–728.
(42) Hehre, W. J.; Ditchfield, R.; Pople, J. A. *J. Chem. Phys.* **1972**, *56*, 2257–2261.
(43) Hariharan, P. C.; Pople, J. A. *Theor. Chim. Acta* **1973**, *28*, 213–222.
(44) Hariharan, P. C.; Pople, J. A. *Mol. Phys.* **1974**, *27*, 209–214.
(45) Gordon, M. S. *Chem. Phys. Lett.* **1980**, *76*, 163–168.
(46) Francl, M. M.; Pietro, W. J.; Hehre, W. J.; Binkley, J. S.; Gordon, M. S.; Defrees, D. J.; Pople, J. A. *J. Chem. Phys.* **1982**, *77*, 3654–3665.
(47) Munk, B. H.; Burrows, C. J.; Schlegel, H. B. *Chem. Res. Toxicol.* **2007**, *20*, 432–444.
(48) Kendall, R. A.; Dunning, T. H.; Harrison, R. J. *J. Chem. Phys.* **1992**, *96*, 6796–6806.
(49) Cances, E.; Mennucci, B. *J. Chem. Phys.* **2001**, *114*, 4744–4745.
(50) Cances, E.; Mennucci, B.; Tomasi, J. *J. Chem. Phys.* **1997**, *107*, 3032–3041.
(51) Mennucci, B.; Tomasi, J. *J. Chem. Phys.* **1997**, *106*, 5151–5158.
(52) Mennucci, B.; Cances, E.; Tomasi, J. *J. Phys. Chem. B* **1997**, *101*, 10506–10517.
(53) Tomasi, J.; Cammi, R.; Mennucci, B. *Int. J. Quantum Chem.* **1999**, *75*, 783–803.
(54) Chipman, D. M. *J. Chem. Phys.* **2000**, *112*, 5558–5565.

Scheme 2. Possible Pathways for Conversion of 8-oxoG, **1**, to 5-OH-OG, **6**

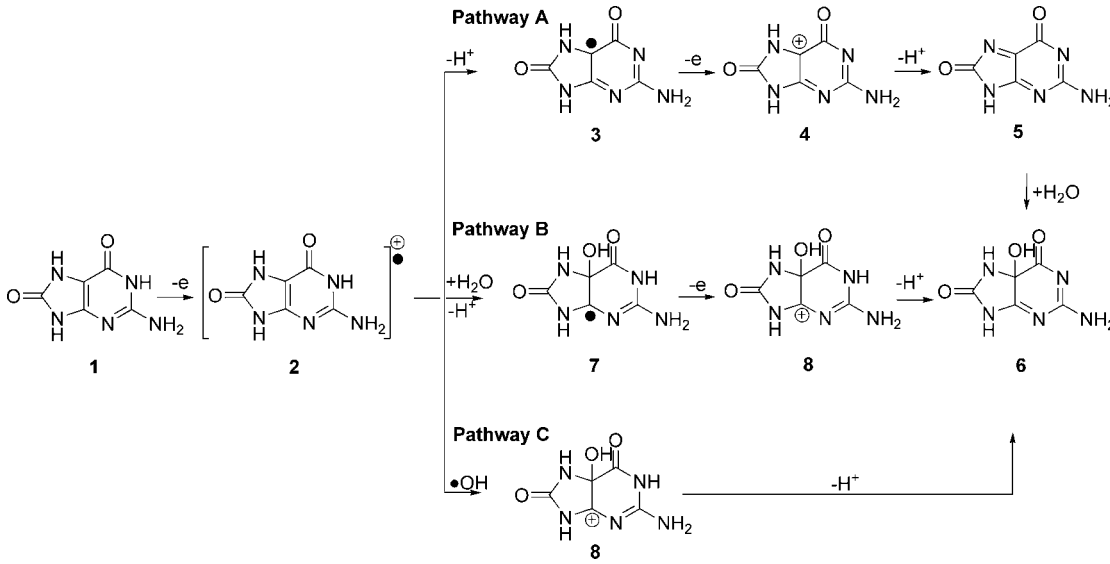

Scheme 3. Possible Pathways for Conversion of 5-OH-OG, **6**, to Guanidinohydantoin (Gh), **12**

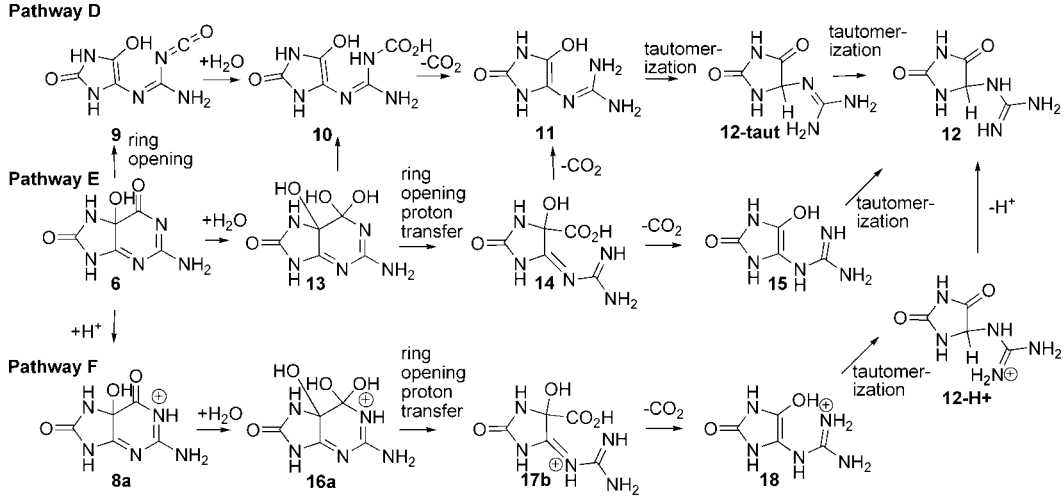

and employed a solvent-excluding surface cavity model, UAKS radii, and tesserae with an average area of 0.200 Å^2. Cartesian coordinates for the optimized geometries and gas-phase energies for the adducts and transition states are provided in the Supporting Information. Vibrational frequencies were computed in the gas phase at the B3LYP level with the 6-31+G(d,p) basis set and were used without scaling since the B3LYP frequencies agree quite well with experimental values for a wide range of second and third period compounds.[55] Thermal corrections and enthalpies were calculated by standard statistical thermodynamic methods[56] using the unscaled B3LYP frequencies and the ideal gas/rigid rotor/harmonic oscillator approximations. The energy in solution for each species is the sum of the electronic energy in the gas phase calculated at B3LYP/aug-cc-pVTZ//B3LYP/6-31+G(d,p), the ZPE at B3LYP/6-31+G(d,p), and the solvation free energy calculated at IEF-PCM/B3LYP/aug-cc-pVTZ//B3LYP/6-31+G(d,p).

The oxidation of 8-oxoG and its adducts has been modeled by transfer of the electron to guanine radical cation to form guanine. Spin contamination was not found to be an issue in any of the open shell calculations (S^2 < 0.77). Mulliken spin densities for the guanine radical cation, the 8-oxoG radical cation, the 8-oxoG(-H) radical, and the 5-OH-8oxoG radical are provided in Supporting Information Figure S1. Geometries for key transition states are shown in Figures 2, 5, 6, 7, and 9. To maintain the charge balance within the calculations, proton transfer between cation adducts was modeled by assuming that the transfer occurs within the 8-oxoG:cytosine base pair producing a protonated cytosine. Between anions the charge balance was maintained by assuming the proton is transferred from the neutral adduct to a methane thiol anion and, conversely, from the neutral methane thiol back to an anion adduct. Methane thiol has been selected as a simple model compound representing anionic biomolecules which may participate in the conversion of 5-OH-OG, **6**, to Sp, **12**.

Results and Discussion

As outlined in Schemes 2, 3, and 4 conversion of 8-oxoG, **1**, to 5-OH-8oxoG, **6**, and ultimately to Gh, **12**, or Sp, **21** can occur via a variety of pathways. The relative energies in solution of

(55) Scott, A. P.; Radom, L. *J. Phys. Chem.* **1996**, *100*, 16502–16513.
(56) McQuarrie, D. A. *Statistical Thermodynamics*; University Science Books: Mill Valley, CA, 1973.

Scheme 4. Possible Pathways for Conversion of 5-OH-OG, **6**, to Spiroiminodihydantoin (Sp), **21**

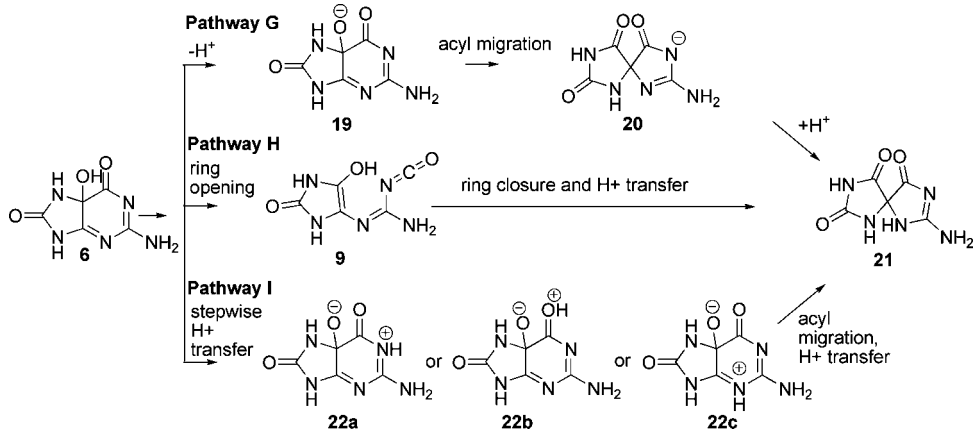

Pathways A−I have been evaluated and are discussed in the paragraphs which follow.

Mechanisms for Formation of 5-OH-OG. Three possible pathways for formation of 5-OH-OG, **6**, from 8-oxoG have been investigated in this study (Scheme 2). All three pathways begin with loss of an electron from 8-oxoG to form the radical cation. This oxidation reaction has been modeled as transfer of an electron from 8-oxoG to guanine radical cation. In an aqueous solution, this reaction is expected to be exothermic by 12.7 kcal/mol based upon the pH 7 reduction potentials of the neutral 8-oxoguanosine (0.74 V) and guanosine radicals (1.29 V).[7] At the level of theory of used in this study, the relative energy in solution of this reaction (1)

$$\text{8oxoG anion} + \text{Guanine radical} \rightarrow \text{8oxoG radical (3)} + \text{Guanine anion} \quad (1)$$

is predicted to be 16 kcal/mol, slightly larger than the free energy difference predicted by the experimental data. In this manuscript, we are comparing the energies of each of the nine pathways relative to each other and this small downward shift of the potential energy surface relative to experiment will have no impact on the conclusions drawn from our data. The gas phase ionization potentials for guanine, 8-oxoG, 8-oxoG(-N1H) and 5-OH-8-oxoGrad were also calculated and are provided in Supporting Information Table S1. The values for guanine and 8-oxoG are similar to the estimates reported in the literature[57–59] and slightly lower than the experimental values.[60,61]

The relative energies in solution for Pathways A, B, and C for the oxidation of 8-oxoG, **1**, to 5-OH-OG, **6**, are provided in Figure 1. Pathways A and B are 2-electron oxidation mechanisms which depend on the presence of an oxidizing species such as a guanine radical cation. Pathway C diverges from Pathway B in the formation of 5-OH-8-oxoG cation, **8**, directly from addition of a hydroxyl radical to 8-oxoG radical cation, **2**. Pathway C may be less significant biologically, since it depends on the localized concentration of hydroxyl radicals within DNA.

Pathways A, B, and C all begin with the transfer of an electron from 8-oxoG to a guanine radical cation. This electron transfer is predicted to be exothermic by 7.5 kcal/mol. For Pathway A, the next step in the mechanism is loss of the N1 proton from the radical cation. This reaction has been modeled as a proton transfer to guanine's Watson–Crick base pair partner, cytosine. Loss of the N1 proton from the radical cation, **2**, to form 8-oxoG radical, **3**, and a protonated cytosine is estimated to be slightly exothermic with a change in energy of 0.7 kcal/mol. These estimates are consistent with the experimentally observed pK_a of 6.6 for 8-oxoG radical cation[7] and similar to published calculations for the proton transfer between either neutral guanine or its radical cation and cytosine. Using solution-phase pK_a data, Steenken[62] estimated that proton transfer from guanine radical cation to cytosine within the G/C base pair was exothermic by 1.5 kcal/mol. In QM/MM calculations conducted on a fully hydrated DNA decamer, Gervasio et al.[63] reported that this proton-transfer reaction was exothermic by 4.0 kcal/mol. The solution-phase forward barrier height for this 8-oxoG radical cation to cytosine proton transfer is predicted to be 8.5 kcal/mol. The calculated barrier height is also in a range consistent with the published estimates of 6−7 kcal/mol for a single proton-transfer reaction between the N1 of guanine and N3 of cytosine in a GC base pair bonded to cisplatin.[64] (For this calculation, Matsui used the B3LYP/LanL2DZ level of theory and the Stuttgart/Dresden ECP for the platinum atom.)

Following loss of the N1 proton from the radical cation **2** to form the 8-oxoG(-H) radical species **3**, the next step along Pathway A is loss of a second electron to form, **4**, the 8-oxoG-(-H) cation. At the level of theory used in this study, the ionization potential for this neutral radical species is slightly higher than the electron affinity of the guanine radical cation due to delocalization of the unpaired electron (Figure S1, Supporting Information), and transfer of this electron is estimated to be endothermic by 5.5 kcal/mol. These calculations are consistent with the work of Steenken,[62] who noted that formation of a neutral radical by proton transfer within the base pair limits the transfer of electrons within the Π backbone of DNA. It is understood that, *in vivo*, the electron may move to a variety of oxidizing species either within the framework of DNA (e.g., bleomycin intercalated into DNA producing superoxide) or electron acceptors in the surrounding environment (e.g., free radical species produced during oxidative stress).[2]

(57) Reynisson, H.; Steenken, S. *Phys. Chem. Chem. Phys.* **2002**, *4*, 527–532.
(58) Wetmore, S. D.; Boyd, R. J.; Eriksson, L. A. *J. Phys. Chem. B* **1998**, *102*, 9332–9343.
(59) Colson, A. O.; Sevilla, M. D. *Int. J. Radiat. Biol.* **1995**, *67*, 627–645.
(60) Hush, N. S.; Chueng, A. S. *Chem. Phys. Lett.* **1975**, *34*, 11–13.
(61) Orlov, V. M.; Smirnov, A. N.; Varshavsky, Ya, M. *Tetrahedron Lett.* **1976**, *48*, 4377–4378.
(62) Steenken, S. *Biol. Chem.* **1997**, *378*, 1293–1297.
(63) Gervasio, F. L.; Laio, A.; Iannuzzi, M.; Parrinello, M. *Chem.-Eur. J.* **2004**, *10*, 4846–4852.
(64) Matsui, T.; Shigeta, Y.; Hirao, K. *J. Phys. Chem. B* **2007**, *111*, 1176–1181.

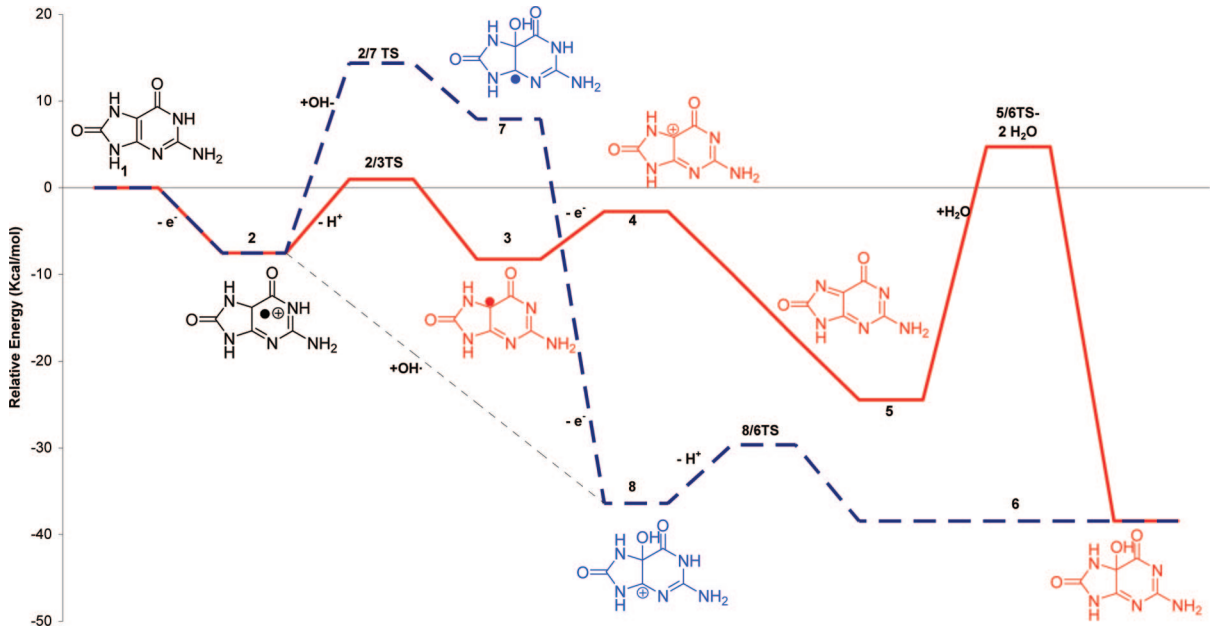

Figure 1. Pathways A, B, and C all begin with the transfer of an electron from 8-oxoG to a guanine radical cation. Relative energy in solution of Pathways A (red solid line), B (blue dashed line), and C (black dotted line) for oxidation of 8-oxoG, **1**, to 5-OH-OG, **6**, calculated at IEF-PCM/B3LYP/aug-cc-pVTZ//B3LYP/6-31+G(d,p). The biological relevance of Pathway C is dependent on the availability of hydroxyl radicals near the DNA backbone. Pathway A may be the kinetically favored biological mechanism.

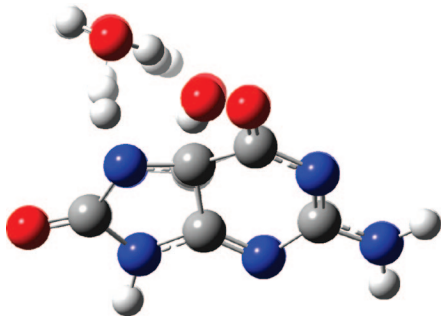

Figure 2. Transition state for the water-assisted hydration of 8-oxoG^{ox}, **5**, to form 5-OH-OG, **6**. Snapshots before the TS, the TS and after the TS are overlaid to indicate motion along the reaction path.

Ⓦ A movie of the molecule along the reaction path is available.

Depending on the electron affinity of these oxidizing species, this reaction could be exothermic *in vivo*. Loss of the N7 proton from **4**, to form 8-oxoG^{ox}, **5**, is predicted to be exothermic by 21.8 kcal/mol. To maintain the charge balance within this calculation, loss of the N7 proton has again been modeled as a proton transfer to cytosine.

Addition of water across the N7−C5 double bond of 8-oxoG^{ox}, **5**, to form 2-amino-5-OH-7, 9-dihydro-purine-6,8-dione (5-OH-OG), **6**, is predicted to be exothermic by 13.9 kcal/mol. The forward barrier height for this reaction was modeled with both one and two explicit water molecules. The barrier height with one water molecule is predicted to be 42.3 kcal/mol. Addition of a second, catalytic, water molecule reduces the barrier height to 29.2 kcal/mol. This 12.9 kcal/mol reduction in the barrier height is likely related to the reduction in ring strain of the transition state when two molecules of water are included. With one explicit molecule of water, the transition state is a four-membered ring; however, with two molecules of water, the transition state is a six-membered ring (Figure 2). The work of Williams et al. on the solvation of carbonyl compounds suggests that additional water molecules may bring the barrier down by a few more kcal/mol.[65] As depicted in the movie, the calculations conducted using the reaction path following algorithms indicate that this reaction proceeds asynchronously with initial protonation of the nitrogen at N7 and subsequent addition of a hydroxide group at C5.

Pathway B begins with conversion of the 8-oxoG radical cation, **2**, to 5-OH-8-oxoG radical, **7**, by net addition of a hydroxide anion. Addition of hydroxide to the C5 position of the radical cation forces the purine to move to a nonplanar geometry and disrupts the conjugation of the π electrons (Supporting Information, Figure S1). Formation of adduct **7** is predicted to be endothermic by 15.4 kcal/mol. Using hydroxide anion to model the transition state for conversion of the radical cation to the 5-OH-8-oxoG radical via nucleophilic addition of water and concerted loss of a proton, the forward barrier height is estimated to be 21.9 kcal/mol.

The 5-OH-8oxoG radical, **7**, can then be oxidized to form the 5-OH-8-oxoG cation adduct, **8**. At the level of theory used in this study, the gas phase ionization potential of adduct **7** is predicted to be 39.1 kcal/mol lower than that of guanine (Supporting Information Table S1). The difference in ionization potential between the two species is likely related to the stability of the delocalized π electrons in the planar guanine relative to the localized π electrons in the nonplanar adduct **7**. Transfer of an electron from **7** to guanine radical cation is predicted to be exothermic by 44.3 kcal/mol. Loss of the N1 proton from the cation, **8**, to form 5-OH-OG, **6**, is predicted to be exothermic by 2.0 kcal/mol. The forward barrier height for transfer of the N1 proton to cytosine is predicted to be 6.7 kcal/mol.

Pathway B could also proceed via addition of hydroxide to the C4 position of the radical cation, **2**, to form 4-OH-OG cation; however, this reaction is also endothermic with a change in energy of 12.9 kcal/mol and a forward barrier height of 30.5 kcal/mol, 8.6 kcal/mol higher than that for addition at the C5 position (Supporting Information, Table S2). The neutral 4-OH-OG adduct formed following deprotonation for the 4-OH-OG cation intermediate is predicted to be 11.9 kcal/mol higher in

energy than 5-OH-OG, **6**, making this pathway kinetically and thermodynamically less favorable than addition at C5.

In Pathway C, 5-OH-8-oxoG cation, **8**, is formed via addition of a hydroxyl radical to 8-oxoG radical cation, **2**, at the C5 position. A variety of approaches were used to identify the transition state for this addition; however, our calculations suggest that this addition may be barrierless at the current level of theory. Addition of a hydroxyl radical at C4 of the radical cation, has a forward barrier height of 6.8 kcal/mol and results in the formation of the 4-OH-8oxoG cation, an adduct which is 25.3 kcal/mol higher in energy than adduct **8** (Supporting Information, Table S2), suggesting again that addition at the C5 position is both kinetically and thermodynamically preferred.

The data suggest that all three pathways are energetically feasible mechanisms for the formation of 5-OH-OG, **6**, from 8-oxoG, **1**. Pathway C is the lowest energy of the three; however, its biological relevance relative to Pathways A and B is dependent on the concentration of hydroxyl radicals near the 8-oxoG radical cation as it is formed. The OH radical is one of the most highly reactive oxygen species produced *in vivo*[66] and can react with a wide variety of biomolecules. Pathway C will be in competition with these other biochemical reactions and may therefore play a smaller role with regard to the production of 5-OH-OG. Pathways A and B are 2-electron oxidation mechanisms and therefore both depend on the local concentration of oxidant. Pathway A may be kinetically favored over Pathway B, as the highest transition state along this pathway, **5/6TS**, is 9.7 kcal/mol lower than the highest transition state along Pathway B (**2/7TS**), and intermediate **3** is 16.1 kcal/mol lower in energy than **7**. The data also suggest that formation of 5-OH-OG is thermodynamically and kinetically preferred to formation of 4-OH-OG.

Mechanisms for Formation of Gh from 5-OH-OG. As outlined in Scheme 3, the solution-phase energetics of three pathways for formation of guanidinohydantoin (Gh), **12**, from 5-OH-OG, **6**, have been explored. Pathway D begins with ring opening to form imidazolidine isocyanate enol intermediate **9** which hydrolyzes to form an imidazolidine enol carbamic acid intermediate **10**. Loss of carbon dioxide from **10** yields an enol imine tautomer **(11)** of Gh. Gh (**12**) is formed from **11** in two steps: an enol/keto tautomerization followed by an imine/amine tautomerization. In Pathway E, 5-OH-OG, **6**, undergoes hydrolysis to form the *gem*-diol intermediate, **13**. This species can undergo ring-opening to a carboxylic acid hydantoin intermediate, **14**. Loss of carbon dioxide from **14**, leads to formation of two possible Gh-enols, **11** and **15**, which then tautomerize to form Gh, **12**. Pathway F differs from Pathway E in that formation of Gh, **12**, from 5-OH-OG, **6**, occurs under acidic reaction conditions which is modeled by having all species protonated.

Conversion of 8-oxoG to Gh and Sp is known to be pH dependent.[9,22,23,67] Slightly acidic conditions favor the formation of Gh over Sp. As a first step in exploring the mechanisms toward formation of either species, the relative energies of 5-OH-OG and its various charged species were calculated (Figure 3). For the protonated species, the positive charge in the relative energy calculations is balanced by assuming that the proton moves from the cytosine cation (CH^+) to neutral

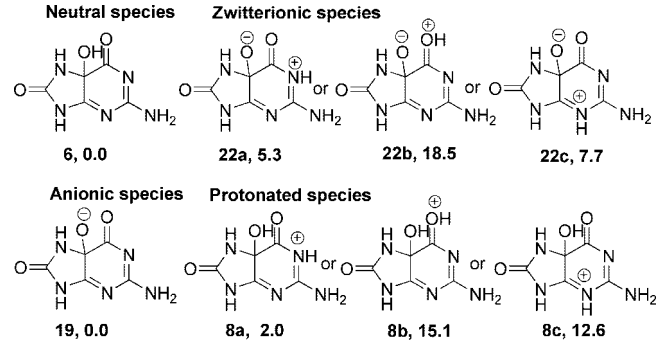

Figure 3. Relative energies in kcal/mol of various tautomeric, protonated, and anionic species of 5-OH-OG. With the exception of **22c**, all data shown are relative energies in solution calculated at IEF-PCM/B3LYP/aug-cc-pVTZ//B3LYP/6-31+G(d,p). For species **22c**, the N3H zwitterion, the electronic energy and free energy of solution were calculated at IEF-PCM/B3LYP/aug-cc-pVTZ// IEF-PCM/B3LYP/6-31+G(d,p). The zero-point energy for **22c** was calculated at B3LYP/6-31+G(d,p)//IEF-PCM/B3LYP/6-31+G(d,p).

5-OH-OG, **6**. For the 5-OH-OG anion, **19**, the calculation assumes that the proton moves from neutral **6** to a CH_3S anion. With the exception of the 5-OH-OG zwitterion protonated at N3, **22c**, all data shown in Figure 3 are relative energies in solution calculated using the gas-phase optimized geometry. For species **22c**, gas-phase geometry optimization resulted in the formation of an epoxide at the C4−C5 bond. The N3H zwitterion was therefore optimized in solution. The data demonstrate a similar trend for the zwitterions and cations as the relative energy in solution increases as the site of protonation moves from the N1 position to N3 to the C6 carbonyl. For the zwitterions, **22a**, with a proton located on N1, is the lowest-energy species with a relative energy in solution versus 5-OH-OG of 5.3 kcal/mol. Similarly, for the cations, **8a**, which is protonated at N1, is the lowest-energy species with a relative energy in solution versus 5-OH-OG of 2.0 kcal/mol. Removal of the proton from the hydroxyl group to form the anion, **19**, is endothermic with an estimated relative energy in solution of 4.6 kcal/mol when methane thiolate is used as the proton acceptor.

The relative energies in solution for the intermediates and transition states along Pathways D, E, and F are provided in Figure 4 and Table S2 of the Supporting Information. Ring opening of 5-OH-OG, **6**, results in the formation of the imidazolidine isocyanate enol intermediate, **9**, and is endothermic by 11.0 kcal/mol with a forward barrier height of 19.1 kcal/mol. Hydrolysis of the isocyanate group gives an imidazolidine enol carbamic acid intermediate, **10**, and is exothermic with a relative energy in solution between the two adducts of 8.5 kcal/mol. The forward barrier height of this reaction is 31.4 kcal/mol when modeled with one reactive and one catalytic molecule of water. Decarboxylation of species **10** yields an imine enol tautomer, **11**, of Gh. This reaction is exothermic by 4.6 kcal/mol and has a water-assisted forward barrier height of 32.8 kcal/mol. Tautomerization of the enol, **11**, to the Gh imine ketone, **12-taut** is exothermic by 23 kcal/mol. These results agree with the experimental observation that the keto form of small molecules is generally more stable than the corresponding enol form. In the case of acetone, the keto form is 12 to 13.9 kcal/mol lower in energy.[68] The forward barrier height modeled with

(65) Williams, I. H.; Spangler, D.; Femec, D. A.; Maggiora, G. M.; Schowen, R. L. *J. Am. Chem. Soc.* **1983**, *105*, 31–40.
(66) Jena, N. R.; Mishra, P. C. *J. Phys. Chem. B* **2005**, *109*, 14205–14218.
(67) Suzuki, T.; Friesen, M. D.; Ohshima, H. *Chem. Res. Toxicol.* **2003**, *16*, 382–389.
(68) Cucinotta, C. S.; Ruini, A.; Catellani, A.; Stirling, A. *ChemPhysChem* **2006**, *7*, 1229–1234.

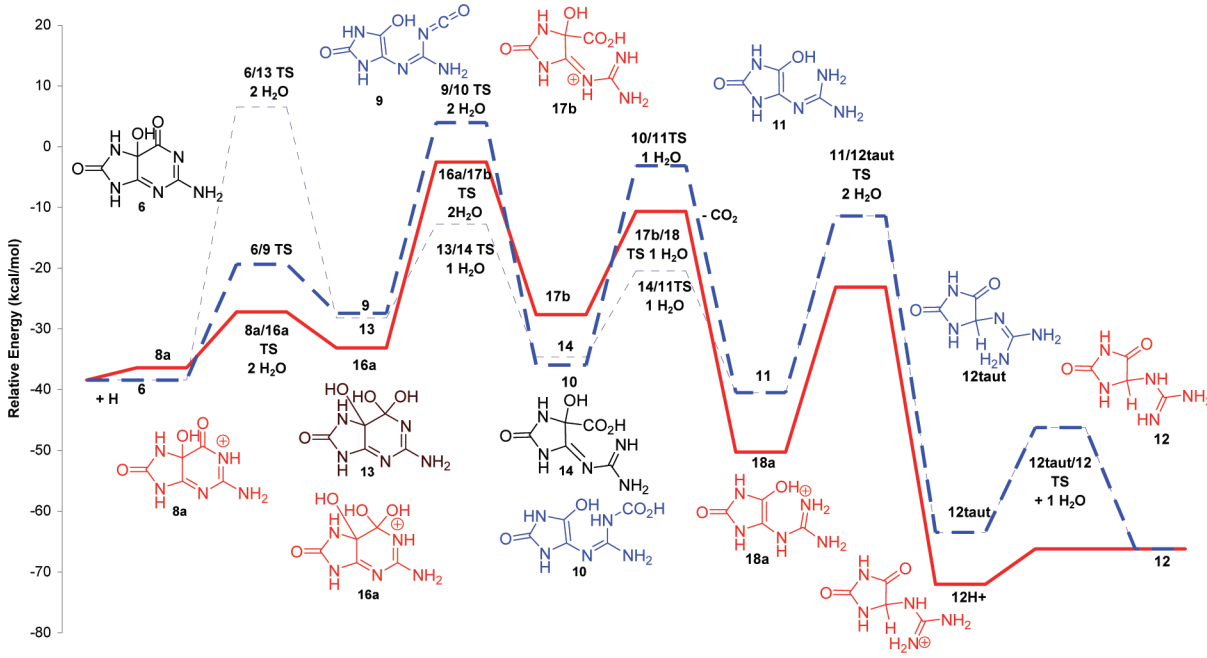

Figure 4. Relative energies in solution of Pathways D (blue dashed line), E (black dotted line) and F (red solid line) for formation of Gh, **12**, from 5-OH-OG, **6** calculated at IEF-PCM/B3LYP/aug-cc-pVTZ//B3LYP/6-31+G(d,p) for all species with the exception of the **6/9TS**. The geometry optimization for the latter transition state was conducted in solution at IEF-PCM/B3LYP/6-31+G(d,p) rather than in the gas phase at the same level of theory. Pathway F is the lowest energy pathway leading to Gh and proceeds via protonation at N1.

two molecules of water is 29.1 kcal/mol which is consistent with published calculations for the keto–enol tautomerization of acetone and in line with the experimental observation that the two Gh diasteromers epimerize at room temperature with a half-life of about 30 min.[8] A study conducted by Lee et al.[69] indicates that addition of one catalytic molecule of water lowered the solution phase barrier height from 73.1 (uncatalyzed reaction) to 45.1 kcal/mol. (This calculation was conducted at the MP2/6-31G(d,p)//MP2/6-31G(d,p) level of theory.) Calculations on the keto–enol tautomerization of acetone conducted by Cucinotta et al. using ab initio molecular dynamics provided a similar barrier height for the reaction catalyzed by one molecule of water and suggest that addition of further water molecules may bring the barrier down by a few more kcal/mol.[68] Based upon the experimental findings of Capon et al., under acidic conditions, the rate for the enol/keto tautomerization, may increase by an order of magnitude, suggesting 1.5–3 kcal/mol decrease in the barrier height for this reaction.[70] The water-assisted tautomerization of the imine, **12-taut**, to Gh, **12**, is slightly exothermic (2.7 kcal/mol) and has an estimated forward barrier height of 17.3 kcal/mol when modeled with one molecule of water. This barrier is likely to be a few kcal/mol lower in the presence of additional molecules of water.

Pathway D could also proceed with the enol/keto tautomerization occurring earlier in the process, however, the calculations indicate that the rate limiting step for this mechanism (**9/9ketoTS**) would be 5.4 kcal/mol higher in energy than the hydrolysis of **9** to form **10**. Data for this higher energy pathway via the keto intermediate are provided in Supporting Information Figure S2 and Table S2.

Pathways E and F differ by whether or not the 5-OH-OG is protonated. Formation of the neutral *gem*-diol, **13**, from 5-OH-OG, **6**, is predicted to be endothermic by 10.2 kcal/mol. For Pathway E, the forward barrier height for the conversion of neutral 5-OH-OG, **6** to the neutral *gem*-diol, **13**, is 53.2 kcal/mol when modeled with one molecule of water. Addition of a second, catalytic molecule of water lowers the barrier to 45.0 kcal/mol. Tautomerization and ring opening of **13** produces a carboxylic acid intermediate, **14**. The relative energy in solution of this exothermic reaction is 6.5 kcal/mol and the forward barrier height modeled with one catalytic water molecule (Figure 6) is 15.4 kcal/mol. This reaction appears to begin with water-assisted transfer of a proton from one of the hydroxyl groups of the *gem*-diol to the N1 position of the pyrimidine ring. Ring opening at the N1−C6 bond follows quickly, yielding the carboxylic acid, **14** (**13** to **14TS**). In an experiment studying

Figure 5. Transition state (TS) for the addition of water to N1 protonated 5-OH-OG, **8a**, to form N1 protonated *gem*-diol intermediate, **16a**, modeled with one reactive and one catalytic molecule of water. Snapshots before the TS, the TS, and after the TS are overlaid to indicate motion along the reaction path.

Ⓦ A movie of the molecule along the reaction path in AVI format is available.

(69) Lee, D.; Kim, C. K.; Lee, B. S.; Lee, I.; Lee, B. C. *J. Comput. Chem.* **1997**, *18*, 56–69.
(70) Capon, B.; Zucco, C. *J. Am. Chem. Soc.* **1982**, *104*, 7567–7572.

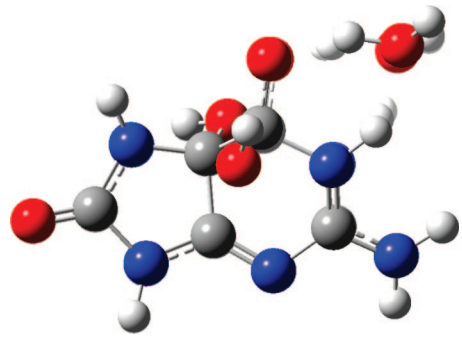

Figure 6. Transition state for water-assisted proton transfer and ring-opening of *gem*-diol intermediate, **13** to form the α-hydroxyl carboxylic acid, **14**. Snapshots before the TS, the TS and after the TS are overlaid to indicate motion along the reaction path.

Ⓦ A movie of the molecule along the reaction path in AVI format is available.

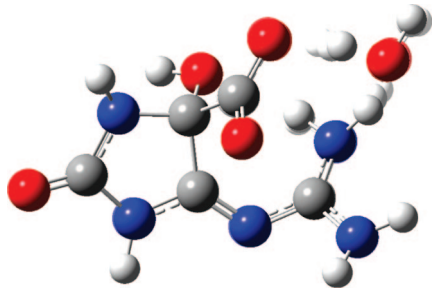

Figure 7. Transition state for water-assisted proton transfer and decarboxylation of **14** to form **11**. Snapshots before the TS, the TS, and after the TS are overlaid to indicate motion along the reaction path.

Ⓦ A movie of the molecule along the reaction path in AVI format is available.

the pathway for conversion of urate to allantoin, a reaction very similar to the conversion of 8-oxoG to Gh, Tipton's group[31] observed that under basic conditions, the reaction proceeded via hydrolysis of the N1−C6 bond, followed by a 1,2 carboxylate shift to form the carbonyl intermediate prior to decarboxylation. Perhaps a similar carboxyl shift could occur under the acidic conditions known to facilitate the formation of Gh. However, this is not the rate-limiting step in the present mechanism.

Cleavage of the C5−C6 bond of the *gem*-diol **13** to form the carbamic acid, **10** under neutral conditions was also evaluated. While this reaction is slightly more exothermic, 7.7 kcal/mol for formation of **10** from **13** vs 6.4 kcal/mol for formation of **14**, it is not kinetically preferred as the forward barrier height is 22.8 kcal/mol, 7.4 kcal/mol higher than the ring opening reaction which forms the carboxylic acid intermediate, **14**. Loss of carbon dioxide from the carboxylic acid intermediate, **14**, produces either Gh-enol **11** or **15** exothermically by 5.9 and 6.9 kcal/mol, respectively. The water-assisted mechanism modeled with one molecule of water has a forward barrier height of 14.2 kcal/mol for formation of **11** and 23.9 kcal/mol for intermediate **15** (Figures 4 and 7, **14** to **11TS** movie).

Formation of the Gh-enol, **11** appears to be the kinetically favored pathway. Tautomerization of **11** to form Gh, **12** proceeds via the mechanism previously discussed for Pathway D. Tautomerization of the Gh-enol, **15**, to Gh, **12**, is exothermic by 24.6 kcal/mol with forward barrier heights of 34.2 and 28.0 kcal/mol when modeled with one and two catalytic water molecules respectively. These barrier heights are about 5 to 10 kcal/mol higher than those predicted for the two-step conversion of the Gh-enol, **11** to Gh, **12**.

Consistent with experimental data indicating that conversion of 8-oxoG to Gh occurs under acidic conditions, our calculations indicate that protonation of **6** reduces the barrier height for the rate-limiting step for this reaction mechanism significantly, making this the kinetically favored pathway. For Pathway F, the relative energies of the first step were calculated for three protonated species, **8a**, protonated at N1, **8b**, protonated at the C6 carbonyl, and **8c**, protonated at N3 (Figure 3 and Table S2 in the Supporting Information). When modeled with one reactant water molecule, the forward barrier heights for formation of the protonated *gem*-diol, **16**, from protonated 5-OH-OG, **8**, are 21.0 kcal/mol for **8b**, 31.8 kcal/mol for **8a**, and 48.4 kcal/mol for **8c**, respectively. Addition of a second, catalytic molecule of water lowered the barrier height for the **8a/16a** transition state to 9.2 kcal/mol, a reduction of 35.8 kcal/mol versus the neutral pathway. A movie depicting the **8a** to **16a** reaction is available. The pathway for this reaction is graphically depicted in Figure 5. The barrier heights for the protonation of species **6** and deprotonation of species **16** have not been calculated but are expected to be on the order of 6–7 kcal/mol based upon the calculations of Matsui et al.[64] for proton transfer reactions within the guanine:cytosine base pair and 6–8.5 kcal/mol based upon our calculations for proton transfer between cytosine and 8-oxoG radical cation, **2**, or 5-OH-OG cation, **8**.

The tautomerization and ring opening of **16** yields a protonated carboxylic acid intermediate, **17**. Calculations were conducted for species protonated at N1, **16a**, and N3, **16b**, and resulting in carboxylic acid intermediates protonated at N1, **17a** and N3, **17b** (Supporting Information, Table S2). The data suggest that the reaction begins by elongation of the N1−C6 bond followed quickly by transfer of a proton from one of the hydroxyl groups in the *gem*-diol to a water molecule forming a hydronium ion. The proton is passed from the hydronium species to either the N1 or N3 position of the ring-opened carbamic acid (**16** to **17TS** movie).

In the latter case, one additional coordinated water molecule assists in the proton transfer. For **16a**, ring opening at the N1−C6 bond is exothermic by 2.5 kcal/mol for **17a** and endothermic by 5.5 kcal/mol for formation of the carboxylic acid intermediate, **17b**. The forward barrier heights are estimated to be 33.5 kcal/mol (modeled with one catalytic water molecule) and 30.6 kcal/mol (modeled with two catalytic water molecules) for conversion of **16a** to **17a** and **17b**, respectively. These barriers are both higher than the 15.4 kcal/mol predicted for conversion of the neutral diol, **13**, to the neutral carboxylic acid intermediate, **14**, via Pathway E. In contrast, ring opening of **16a** at the C5−C6 bond to yield a carbamic acid protonated at N3, **10N3H**$^+$, is exothermic by 2.0 kcal/mol but has a forward barrier height of 36.4 kcal/mol making it kinetically less favored. Ring opening of **16b** to form **17b** is exothermic by 7.9 kcal/mol and has a forward barrier height with one catalytic water molecule of 13.4 kcal/mol, 2.1 kcal/mol lower than the barrier height of the unprotonated pathway (**13** to **14** TS). Proton transfer and decarboxylation of either **17a** or **17b** leads exothermically to formation of the protonated Gh-enol, **18**, by 14.7 and 22.7 kcal/mol, respectively. The calculations indicate that the protonated intermediate, **18**, is 8.7 and 9.8 kcal/mol more stable than the unprotonated Gh-enols, **15** and **11**. When modeled with one catalytic molecule of water, the forward barrier heights are 16.9 kcal/mol for **17b** to **18** and

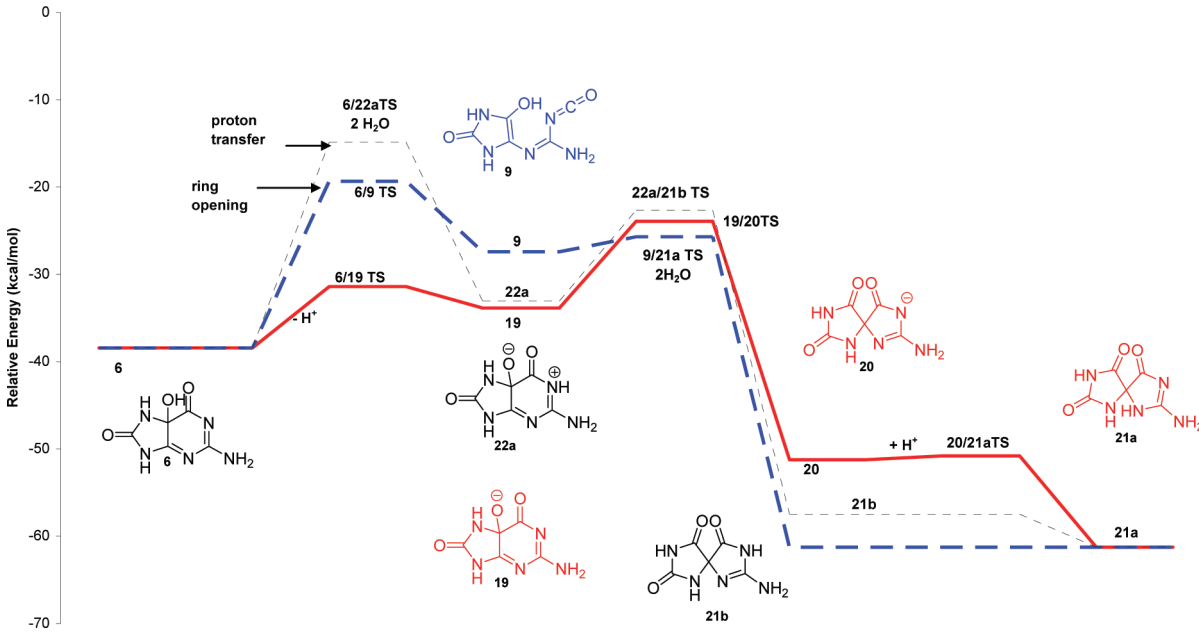

Figure 8. Relative energy in solution of Pathways G (red solid line), H (blue dashed line) and I (black dotted line) for formation of Sp, **21**, from 5-OH-OG, **6** calculated at IEF-PCM/B3LYP/aug-cc-pVTZ//B3LYP/6-31+G(d,p) for reactants and products. Geometry optimization for **6/9TS**, **19/20TS**, and **22a/21bTS** was conducted in solution at IEF-PCM/B3LYP/6-31+G(d,p) rather than in the gas phase at the same level of theory. Consistent with experiment suggesting that formation of **21** is facilitated by basic conditions, Pathway F via the anion intermediate, **19**, is energetically lower than the mechanisms proceeding through zwitterionic or uncharged species.

26.0 kcal/mol for **17a** to **18**, slightly higher than the barrier heights for decarboxylation of the neutral species, **14**. Enol/keto tautomerization of **18** leads yields protonated Gh and is exothermic by 21.7 kcal/mol with a forward barrier height modeled with one water molecule of 27.2 kcal/mol, 2 kcal/mol lower than the barrier height obtained for tautomerization of the neutral species. The data suggest that the protonated form of Gh is 5.8 kcal/mol more stable than the unprotonated form of Gh, **12**.

Of the three pathways studied, Pathway F is the lowest energy path leading to formation of Gh, **12** from 5-OH-OG, **6**, due to the substantial reduction in the barrier height for formation of the *gem*-diol when **6** is protonated at N1. Pathway D may be kinetically preferred to Pathway E for the neutral molecule as the barrier height for its rate limiting step is 2.6 kcal/mol lower in energy.

Mechanisms for Formation of Sp from 5-OH-OG. Three possible mechanisms for conversion of 5-OH-OG, **6**, to spiroiminodihydantoin (Sp), **21**, have been examined (Scheme 4). Given the experimental data showing that formation of Sp is favored by a higher pH environment, Pathway G begins with the loss of a proton to form the 5-OH-OG anion, **19**. Migration of the acyl group to the C4 carbon produces the Sp anion, **20**, which is then protonated to form the neutral compound, **21**. In Pathway H, 5-OH-OG, **6**, opens to form a neutral imidazolidine enol isocyanate intermediate, **9**. The enol, **9**, then undergoes concerted proton transfer and ring closure to form Sp, **21**. The third mechanism forms Sp, **21**, from 5-OH-OG, **6**, via proton transfer and acyl migration stepwise via a zwitterion (Pathway I).

For Pathway G, loss of a proton from 5-OH-OG, **6**, produces the anion, **19**, endothermically with a 4.6 kcal/mol change in the relative energy in solution when methane thiol anion is used as the model for the proton acceptor (Supporting Information Table S4, Figure 8). The barrier height is predicted to be 7.0 kcal/mol which is in a range consistent with similar proton transfers in the present work. Pathway G continues with migration of the C6 acyl group to C4 to form the Sp anion, **20** (Figure 9).

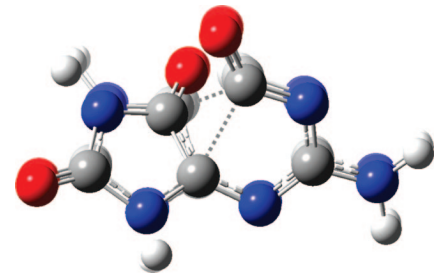

Figure 9. Transition state for acyl migration of C-6 carbonyl group in **19** to form Sp anion, **20**. Snapshots before the TS, the TS and after the TS are overlaid to indicate motion along the reaction path.

Ⓦ A movie of the molecule along the reaction path in AVI format is available.

This motion is depicted in the **19 to 20 TS** movie (see Figure 9). Formation of this anion is estimated to be exothermic by 17.4 kcal/mol with a forward barrier height of 9.9 kcal/mol. Protonation of the Sp-anion, **20**, at N3 to form Sp, **21a**, is estimated to be exothermic by 10.1 kcal/mol and nearly barrierless with a forward barrier height of 0.4 kcal/mol. As shown in Figure 10, protonation of **20** at other sites produces adducts with higher energies relative to **21a**.

Pathway H begins with the endothermic ring opening of 5-OH-OG, **6**, to form the imidazolidine enol isocyanate intermediate, **9.** As noted previously, formation of **9** is endothermic by 11.0 kcal/mol with a forward barrier height of 19.1 kcal/mol. This species is stabilized by the formation of a partial single bond (1.62 Å) between C6 of the isocyanate and C4 of the imidazolidine ring. As the C4−C6 distance decreases, this ring-opened species can undergo coordinated water-assisted proton transfer and ring closure to form Sp, **21**. This reaction is exothermic by 33.9 kcal/mol with a forward barrier height of

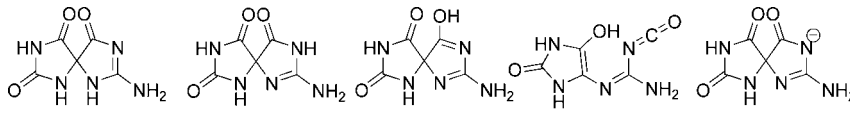

Figure 10. Relative energies in kcal/mol of various isomers of spiroiminodihydantoin. Data shown are relative energy in solution calculated at B3LYP/aug-cc-pVTZ//B3LYP/6-31+G(d,p) using the IEF-PCM solvation model.

1.7 kcal/mol. The transition state for this reaction was modeled with two explicit molecules of water.

As shown in Figure 3, the proton from the C5 hydroxyl group can be transferred to one of three sites on 5-OH-OG, **6**, to form the zwitterions **22a**, protonated at N1, **22b**, protonated at the C6 carbonyl oxygen, and **22c**, protonated at N3. This water-assisted proton transfer reaction is endothermic for all three zwitterions (Figure 3, Supporting Information Table S4) with the smallest forward barrier height, 23.6 kcal/mol, predicted for the transition from **6** to **22a** modeled with two catalytic molecules of water. With one catalytic molecule of water, the barrier heights are 28.4 kcal/mol, 24.1 kcal/mol, and 39.7 kcal/mol for the transition from **6** to **22a**, **22b** and **22c**, respectively. Addition of a second molecule of water reduces the **6** to **22c** barrier height by 6.1 kcal/mol. Migration of the C6 acyl group of **22a** to C4 yields the Sp isomer **21b** and is predicted to be exothermic by 24.4 kcal/mol. The forward barrier height for this reaction is predicted to be 10.4 kcal/mol. Formation of Sp isomers **21c** and **21a** from zwitterions **22b** and **22c** is predicted to be exothermic by 21.8 and 30.6 kcal/mol, respectively. The forward barrier heights for these two acyl migrations are calculated to be 13.6 kcal/mol for the conversion of **22b** to **21c** and 12.2 kcal/mol for the **22c** to **21a** transition. As noted previously, proton transfer from either the N1 or C6 site of Sp to N3 occurs exothermically to give the **21a** tautomer. While this reaction is expected to be facile in solution, we were unable to identify the transition state for proton transfer from N1 to N3 even with one to three explicit molecules of water.

At the present level of theory, the mechanism for the proton transfer and acyl migration from neutral 5-OH-OG, **6**, to form Sp, **21**, or one of its isomers appears to proceed in a stepwise fashion. Searches for a concerted transition state involving at least one explicit molecule of water were unsuccessful in both the gas and solution phases. The calculations to date suggest that the neutral reaction proceeds via either Pathway H, ring-opening followed by proton transfer and ring closure, or via Pathway I, initiated by proton transfer followed by acyl migration.

Consistent with experimental data showing that formation of Sp is facilitated by basic conditions, Pathway G via the anion intermediate, **19**, appears to be the kinetically favored mechanism as its highest forward barrier (**19/20TS**) is at least 9 kcal/mol lower than the highest barriers proceeding through zwitterionic or uncharged species.

Effect of pH on the Formation of Gh and Sp. As noted previously, the product distribution of Gh, **12** and Sp, **21**, varies with pH with formation of Gh favored at pH < 6 and Sp favored at pH > 7.[23] As shown in Figures 4 and 8, our calculations are consistent with these findings. Under basic conditions, Pathway G, for Sp via the 5-OH-OG anion, **19**, is kinetically favored over the either the neutral or protonated pathways for Gh as the rate limiting step is at least 8 kcal/mol lower in energy than that of the other pathways. For the neutral molecule, the highest barrier height for formation of Sp (**6/22aTS**) via Pathway I is 21.4 kcal/mol lower than highest barrier height for the production of Gh via Pathway E (**6/13TS**) and 18.8 kcal/mol lower than the highest barrier height along Pathway D (**9/10TS**). These data are consistent with the experimental observation that the Gh/Sp product ratio is 3:52 at pH 7.[23] At pH 4.5, the Gh/Sp product ratio is approximately 40:1 suggesting that the rate limiting barrier height (**17b/18TS**) via Pathway F for Gh is a few kcal/mol lower than that of the rate limiting barrier heights along a protonated variant of either Pathways H or I for Sp.

Conclusions

The potential energy surface for formation of 5-OH-OG, **6**, Gh, **12** and Sp, **21**, from 8-oxoG, **1**, has been mapped out using DFT and the IEF-PCM model for solvation.

8-oxoG to 5-OH-OG. Three pathways were evaluated for the formation of 5-OH-OG, **6**, from 8-oxoG, **1**. The data suggest that all three pathways are energetically feasible mechanisms. Pathway A, sequential loss of two electrons and two protons to form 8-oxoG^{ox}, **5**, followed by hydration to yield 5-OH-OG, may be kinetically favored over Pathway B. Both Pathways A and B depend on the local concentration of oxidizing agent. Pathway C, involving hydroxyl radical addition to the 5-OH-8-oxoG cation, while lower in energy than either A or B, will be in competition with other biochemical reactions for the reactive oxygen species, OH•, and may play a smaller role in the production of 5-OH-OG.

5-OH-OG to Gh and Sp. Six pathways were considered for the formation of Gh, **12**, and Sp, **21**, from 5-OH-OG, **6**. Pathways D and E outlined formation of Gh for the neutral molecule and differed in the cleavage of either the C5−C6 bond or N1−C6 bond and the timing of the hydrolysis of the intermediate to a carboxylic or carbamic acid. Pathway F evaluated the effect of protonation on the energetics of Pathway E. Pathways G, H, and I explored the formation of Sp via anionic, neutral and zwitterionic intermediates.

Cleavage of C5−C6 vs N1−C6 bond. For the neutral molecule, formation of Gh from 5-OH-OG is kinetically more likely to proceed via cleavage of the C5−C6 bond (Pathway D) rather than via cleavage of the N1−C6 bond (Pathway E). Experimentally, amide hydrolysis is known to be facilitated by strong acid or base. Our data indicate that protonation of 5-OH-OG (Pathway F), reduces the barrier heights for cleavage of the N1−C6, bond making it the kinetically favored pathway.

Effect of pH on Formation of Gh or Sp. The data are consistent with experimental findings showing a dependence of the Gh/Sp product ratio on the reaction pH. Under neutral and basic conditions, formation of Sp, **21**, via an anion intermediate (Pathway G) is kinetically favored over Pathways D, E, and F for formation of Gh, **12**. Under acidic conditions, Gh, **12**, is predicted to be the kinetically favored product.

Overall, these studies help decipher the most likely pathways available during 8-oxoG oxidation by sequential one-electron abstraction leading ultimately to the hydantoin products Sp and Gh. The precise pathway followed is shown to depend on pH of the medium, as well as oxidant concentration; however, the nature of the nucleophile may also play a key role in determining the precise timing of nucleophilic attack with respect to

oxidation and proton-transfer steps. The current study in which the nucleophile is water (or hydroxide) has presented a clearer picture of the mechanisms of formation of the parent heterocycles, Sp and Gh, and may serve as a basis for understanding a broader class of hydantoin adducts such as those formed in the presence of amines or other nucleophiles including protein side chains.[71]

Acknowledgment. This work was supported by grants from the National Science Foundation (CHE 0512144 to H.B.S., CHE 0514612 to C.J.B.). We thank C&IT, ISC, and the Department of Chemistry at Wayne State University for computer time.

Supporting Information Available: The molecular geometries in Cartesian coordinates, the solution phase relative energies for all adducts and corresponding transition states, the Mulliken spin densities for open-shell species, and the complete reference 37. This material is available free of charge via the Internet at http://pubs.acs.org.

JA7104448

(71) Johansen, M. E.; Muller, J. G.; Xu, X. Y.; Burrows, C. J. *Biochemistry* **2005**, *44*, 5660–5671.